Performance and reliability of PZT-based piezoelectric micromirrors operated in realistic environments

R. P. Dahl-Hansen[1,2*], T. Tybell[1]
[1]Norwegian University of Science and Technology
Department of Electronic Systems,
7491, Trondheim, Norway

F. Tyholdt[2]
[2]SINTEF Digital, MiNaLab,
Gaustadalleen 23C, 0373, Oslo, Norway
*runarplu@ntnu.no

***Abstract*—The number of application areas for piezoelectric microelectromechanical systems based on PZT have increased rapidly over the years. Thus, to continue the development towards commercial deployment, characterizing lifetime and reliability during operation in realistic and harsh environments is important. Such environments are demanding for piezoMEMS devices since they often involve high humidity levels and elevated temperatures which gives rise to complex degradation. To address how such conditions affects device performance we combined optical and electrical measurements to elucidate the degradation of a PZT-based thin-film piezoelectric MEMS micromirror during temperature-humidity-cycling tests. As a test structure, $1\ \mu m$ $PbZr_{0.40}Ti_{0.60}O_3$ on a $10\ nm$ $LaNiO_3$ buffer-layer, were deposited by pulsed laser deposition on platinized Silicon-on-Insulator wafers. A 250 nm Au/TiW top electrode was deposited by DC-sputtering before structuring the final device. The micromirrors were unipolarly actuated with a signal of $20\ V$ peak-to-peak at a frequency of $1.5\ kHz$ in an ambient with constant vapor concentration of $22\ g/m^3$ for device temperatures between $25\ ^oC$ and $175\ ^oC$. Humidity-related degradation was manifested as local breakdown events and pinholes on top of and along the edges of the used electrodes. This had a strong effect on device performance and preceded degradation due to polarization-fatigue at all temperatures. Also, both the initial piezoelectric response and number of cycles to device failure increased with increasing substrate temperature in humid ambient.**

Keywords: PiezoMEMS reliability, lifetime, fatigue, temperature, humidity

I. INTRODUCTION

Due to its large piezoelectric response, $PbZr_xTi_{1-x}O_3$ (PZT) is commonly used for piezoelectric microelectromechanical systems (piezoMEMS) including RF-switches, ultrasonic transducers, gas sensors and micromirrors [1], [2]. Prior to commercialization, cycling tests in humid ambient and at elevated temperatures are important to assess the reliability of piezoMEMS-devices operated in realistic and harsh environments. Device operation in high humidity are associated with the early onset of irreversible degradation, including elemental migration, cracking and local breakdown events [3]. This primarily occurs in close vicinity to the used electrodes and originates from electrical, mechanical and electrochemical processes occurring both within PZT and on the PZT and electrode surfaces during operation. Elevated temperatures on the other hand will impact the reversible degradation mechanisms due to changes in the dielectric and piezoelectric properties, as well as increase the leakage and change the stress-strain relations of the structure [4]–[6]. Since thin-film piezoMEMS-devices in general rely heavily on the stress-transfer between the film and substrate, in-plane changes caused by any such degradation may have major implications on the electromechanical response and therefore the device performance. Hence it is important to assess how the piezoelectric response, lifetime and reliability of each piezoMEMS-device is affected by elevated temperature and ambient humidity.

In the current work we investigated the degradation and electromechanical response of bimorph PZT-based thin film micromirrors during operation in humid ambient and elevated temperatures.

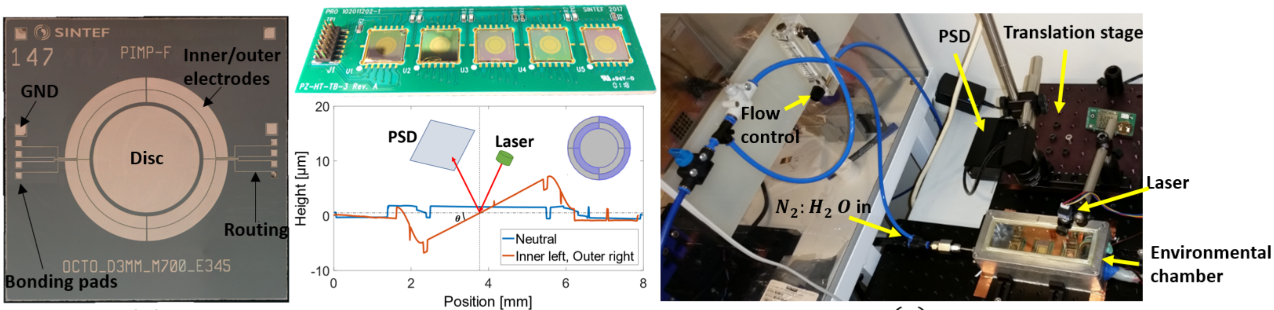

(a) (b) (c)

Figure 1: Device and experimental setup. (a): structure of the tested micromirror, (b): MEMS test-circuit for simultaneous testing of five micromirrors and actuation giving the maximum 2D tilt of $\pm 0.5^o$ The laser was reflected of the mirror onto a position sensitive device (PSD). (c): environmental chamber and experimental setup. The ambient was kept constant with an absolute humidity of 22 g/m^2 and the micromirrors were heated from below by a hot-plate.

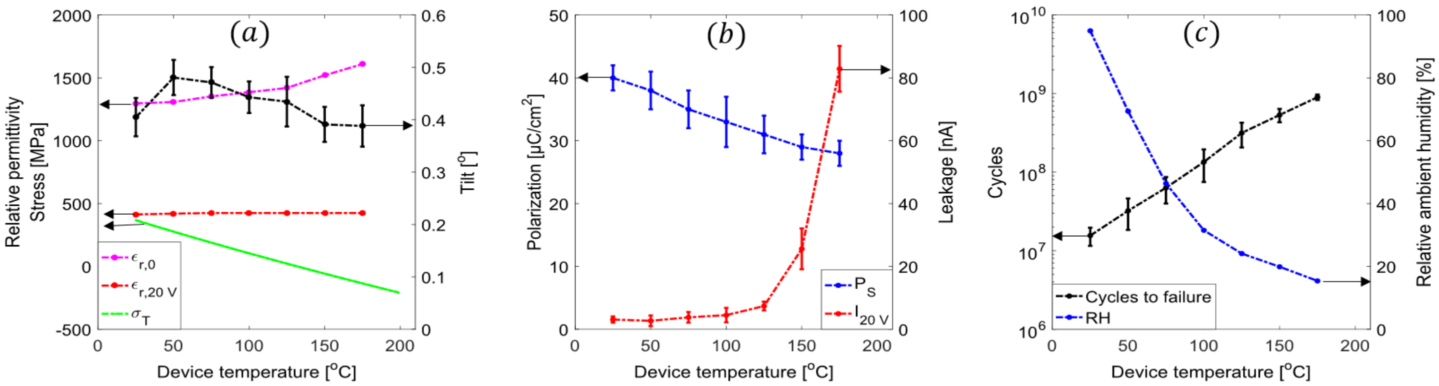

Figure 2: (a): Measured relative permittivity at 0 V, $\varepsilon_{r,0}$, and 20 V, $\varepsilon_{r,20\,V}$, calculated thermal stress, σ_T, and deflection tilt as a function of device temperature. (b): average polarization and leakage as a function of device temperature. (c): Average cycles to failure, and relative humidity due to heated ambient as a function of device temperature.

II. Methods

Piezoelectric micromirrors, see *Fig. 1* (a), were fabricated according to literature [1] using 1 µm pulsed laser-deposited Ba-doped $PbZr_{0.40}Ti_{0.60}O_3$. The mirror consisted of a rigid Silicon disc $3\,mm$ in diameter, suspended on a flexible membrane surrounded by eight integrated PZT-actuators. 2D tilt and out-of-plane movement was enabled by actuating the inner and outer electrodes according to *Fig. 1* (b). For the micromirrors used in this work, a maximum 2D tilt of $\pm 0.5^o$ was achieved by simultaneously actuating the two inner and two outer electrodes on opposite sides of the center disc. Five micromirrors were wire-bonded to a test-circuit and actuated in parallel inside the environmental chamber for each test condition. The ambient vapor concentration was kept constant at $22\ g/m^3$ by bubbling N_2 through a DI-water container and introducing the mixture into the chamber as shown in *Fig. 1* (c). Humidity and ambient temperature (T_{atm}) was measured using a HYT271 humidity-sensor and the micromirrors heated from below by a hotplate. The micromirror temperature (T_{sub}) was measured using a k-type thermocouple attached to the surface of one of the tested devices.

After ambient stabilization, the micromirrors were unipolarly actuated with a peak-to-peak voltage (V_{PP}) of $20\ V$ at $1.5\ kHz$ while T_{sub} was varied in steps of $25\ ^oC$ from $25\ ^oC$ to $175\ ^oC$. A laser was reflected of the micromirror through an optical window onto a position sensitive device (PSD) for electromechanical characterization. The recorded x -and y-positions of the laser trace were then used to approximate the deflection tilt according to:

$$tan(2\theta) \approx 2\theta = \frac{\sqrt{x^2 + y^2}}{l}\ [rad] \qquad (1)$$

where θ is the achieved angular deflection of the micromirror according to the neutral plane, see *Fig. 1* (b), and l the length from the device to the PSD. Ferroelectric characterization was done by retrofitting an aixACCT TF2000 Analyzer to the experimental setup. Ferroelectric hysteresis was measured at $10\ Hz$ with a large-signal of $-25\ V$ to $25\ V$, the capacitance-measurements with a small-signal amplitude of $200\ mV$ at $1\ kHz$ and the leakage with steps of $2\ V$ and $2\ sec$ dwell from $-20\ to\ 20\ V$.

III. Results and Discussion

A. *Electromechanical response*

Fig. 2 (a) show the measured average angular tilt, relative permittivity at 0 V ($\varepsilon_{r,0\,V}$) and 20 V ($\varepsilon_{r,20\,V}$) and calculated total thermal stress in the device stack (σ_T) plotted as a function of T_{sub}. The measured average saturation polarization (P_S) and leakage at $20\ V$ ($I_{20,V}$) is shown in *Fig. 2* (b) and the values summarized in *TABLE I*. $\varepsilon_{r,0}$, $\varepsilon_{r,20\,V}$ and $I_{20\,V}$ increases, while P_S decreases with increasing T_{sub} and is consistent with literature on ferroelectrics [5]. As shown in *Fig. 2* (a) the measured average tilt increases with T_{sub} and peaks at 50^oC before it decreases for $T_{sub} > 50\ ^oC$. Such electromechanical behavior has also been reported for similar PZT-based ceramics in literature [7]. Thin-film devices such as the present micromirror, are particularly sensitive to the in-plane circumstances. Hence in-plane stress, excitation field and device geometry are important for the final electromechanical response. The bending moment moving the current device structure originates from the total in-plane stress (σ_{tot}) and has three main contributions: the residual stress (σ_R) applied stress (σ_A) and piezoelectric stress (σ_P). The latter being the controllable stress, relates to the

TABLE I: Average Measured Values

Device	$T_{sub}\ [^oC]$	$T_{atm}\ [^oC]$	***Tilt*** $[deg]$	***Cycles to failure***	$\varepsilon_{r,0}$	$\varepsilon_{r,20}$	$P_R\ [\frac{\mu C}{cm^2}]$	$P_S\ [\frac{\mu C}{cm^2}]$	$I^+\ [nA]$	$\sigma_T\ [MPa]$	RH [%]
$1-5$	25	25.0	0.40 ± 0.04	$1.6x10^7 \pm 0.4x10^7$	1297	414	10.3	40 ± 2	3.1 ± 1.0	*368*	95.0
$6-10$	50	30.8	0.48 ± 0.03	$3.2x10^7 \pm 1.4x10^7$	1308	420	10.3	38 ± 3	2.7 ± 1.7	*284*	69.4
$11-15$	75	38.5	0.47 ± 0.03	$6.3x10^7 \pm 2.3x10^7$	1353	424	9.3	35 ± 3	3.8 ± 1.7	*196*	46.4
$16-20$	100	46.4	0.44 ± 0.03	$13.5x10^7 \pm 6.0x10^7$	1387	425	8.3	33 ± 4	4.5 ± 2.3	*111*	31.5
$21-25$	125	52.1	0.43 ± 0.04	$31.6x10^7 \pm 10.9x10^7$	1420	425	7.9	31 ± 3	7.4 ± 1.4	*29*	24.1
$26-30$	150	56.4	0.40 ± 0.03	$53.5x10^7 \pm 10.4x10^7$	1521	425	8.0	29 ± 2	25.6 ± 6.5	*-51*	19.9
$31-35$	175	62.3	0.39 ± 0.04	$90.0x10^7 \pm 7.2x10^7$	1610	425	8.0	28 ± 2	82.9 ± 7.3	*-129*	15.4

TABLE II: VALUES FOR THERMAL STRESS CALCULATION

Material	$E\,[GPa]$	ν	$\alpha x10^{-6}\,[K^{-1}]$	$T_{dep}\,[^oC]$	*Ref.*
Au	*78*	*0.44*	*14.2*	*25*	*[5]*
PZT	*161*	*0.31*	*6*	*620*	*[5]*
Pt	*168*	*0.38*	*9*	*450*	*[5]*
SiO_2	*70*	*0.3*	*0.6*	1050	*[5]*
Si	*170*	*0.28*	$-15.2459 + 3.43026\ln(T)$	*N/A*	*[8]*

transverse electric field, E_z, and the effective in-plane piezocoefficient, $e_{31,f}$ by $\sigma_P = -e_{31,f}E_z$. $e_{31,f}$ is proportional to P_S and ε_r measured out-of-plane (along the 3-direction), i.e. $e_{31,f} \propto -2\varepsilon_{33}P_3$ [5]. Since the relative decrease in P_S seems to be larger than the relative increase in $\varepsilon_{r,0}$ and $\varepsilon_{r,20}$, the net σ_P (and total deflection) is expected to decrease with increasing temperature. From the measured values of P_S and ε_r, this should correspond to a net decrease of the total in-plane stress by 4.2 % at 50^oC. On the contrary, the measured initial deflection is indeed increasing by 20 % from 25 ^oC to 50 ^oC, and remains larger than the room-temperature deflection up to $T_{sub} = 175\,^oC$. We suggest that this is partly due to stress changes in the stack where $\sigma_{tot} = \sigma_R + \sigma_A + \sigma_P$. A large portion of the residual stress is the thermal stress between the film and substrate given by:

$$\sigma_T = \frac{E_{film}\left(\alpha_{film} - \alpha_{sub}\right)\Delta T}{\left(1 - \nu_{film}\right)}\,[MPa] \qquad (2)$$

where α is the thermal expansion coefficients of the used materials, E_{film} is the Young's modulus, ν_{film} is the Poisson ratio and ΔT is the difference between the deposition and T_{sub}. Here a positive sign corresponds to a tensile stress and a negative sign to a compressive stress. As a simple first order approximation, σ_T was calculated for the adjacent films and added together for the entire stack (for exact stress-calculations of multi-layered stacks, the thickness and device geometry must also be considered). The linear thermal expansion coefficient was used for all materials except Si which displays the largest nonlinearities in the relevant temperature range [8]. *TABLE II* summarizes the used thermal expansion values and the calculated σ_T at the different T_{sub} can be found in *Fig. 2* (a) and *TABLE I*. Despite the simplicity of the used model the calculated stresses correlate well with measured values from previous wafer bending experiments.

PLD-deposited PZT typically holds a substantial amount of residual stresses post processing causing a reduction in the piezoelectric response. As T_{sub} increases, the thermal contribution to this stress stress is gradually relaxed, which will move the operation point away from the saturation point in the piezoelectric hysteresis. Due to increased linearity, any such stress-relaxation is expected to increase the piezoelectric response which is indeed observed here. Also, the highly nonlinear α of Silicon will in the current temperature range cause the largest thermal stress-relaxation of the stack to occur between 25^oC and 100^oC and may therefore be an additional contribution. Also, it can be mentioned that increased domain wall mobility with temperature will have a positive effect on the unipolar strain [6].

B. Humidity-related degradation

Micrographs of the bonding pads after device failure is shown in *Fig. 3* (a). Humidity-related degradation was primarily manifested as local breakdown-events and pinhole-formation along the edges and on top of all utilized top electrodes. The ground pads and unused electrodes, however, remained unaffected. As shown in *Fig. 3* (a), the relative pinhole concentration appeared to be considerably larger along the electrode edges than on top of the electrode surfaces. Also, the total number and relative portion of pinholes along the edges compared to the electrode surface was significantly larger at lower T_{sub} than at higher T_{sub}. Since for the present experiments the applied voltage was above the standard potential for catalytic water-splitting of $1.23\,V$, we speculate that water-splitting catalysis can facilitate the observed degradation. During testing, the Ti/W-layer used as an adhesion-layer between Au and PZT was exposed to the ambient along the electrode edges and can hence form catalytically active oxides such as TiO_2 and WO_3 in the presence of humidity. If water-splitting is indeed occurring, hydrogen will evolve on the top electrode and may quickly diffuse into PZT along the electrode edges. If e.g. hydrogen-induced hardening reduces the critical stress (the maximum stress the PZT-films can accommodate before cracking) so that the application of σ_P results in cracks, the edges should be affected first by such degradation. The fact that the unused and bottom electrodes remains unaffected may indeed further support this claim and similar observations have been reported for PZT under DC-bias [9], [10] and in the FERAM-literature [11].

For water splitting to occur on the electrode surface, PZT should either be exposed through the top electrode or catalysis should occur on the Au. The former can be true in the presence of pinholes, large local defects such as sputtered particles or cracks appearing during operation. The latter have recently caught interest in literature due to the catalytic activity of gold [12]. To understand the connection of the observed degradation to elevated temperatures, the adsorption of water on the device

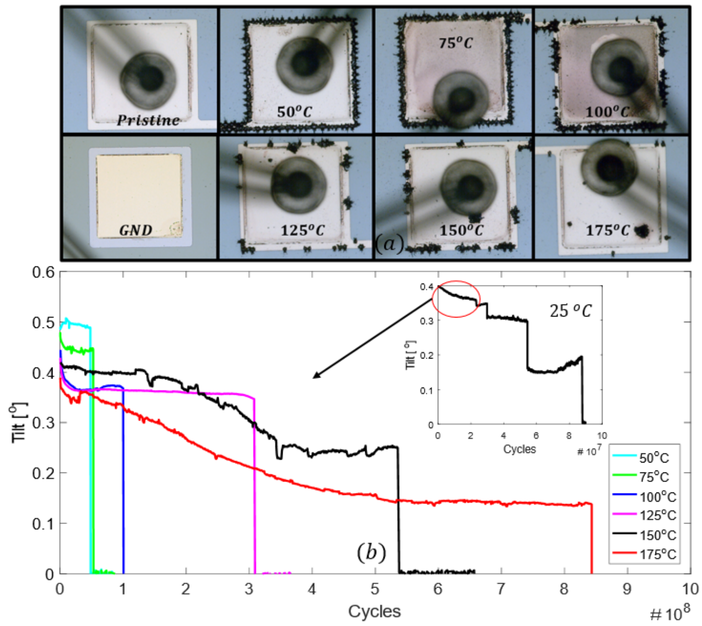

Figure 3: (a): micrographs of bonding pads after failure at $25 - 175^oC$ in humid ambient and (b): measured deflection as a function of cycles.

surface must be discussed. In humid ambient, the surface of perovskite oxides, including PZT, will quickly saturate with a thermally stable layer of chemisorbed hydroxide species and PZT is therefore by itself assumed not to be severely affected by humidity in the absence of applied voltages, e.g. far away from the used electrodes [13]. Gold on the other hand, is chemically inert and will facilitate molecular adsorption of water [14]. The number of adsorbed molecules depend on the heat of adsorption and desorption of water at a given relative humidity (RH) and T_{atm}. For $RH < 60\%$ the water adsorbed on gold can be approximated by the Brunauer–Emmett–Teller (BET) theory:

$$M_W = \frac{cRH}{(1-RH)(1+RH(c-1))} \left[\frac{\mu\boldsymbol{g}}{\boldsymbol{cm^2}}\right] \qquad (3)$$

Here M_W is the number of adsorbed monolayers, $c = e^{\frac{Q_i - Q_v}{RT_i}}$ a material-related constant, Q_i and Q_v the heat of water adsorption and desorption, R the universal gas constant and T_i the temperature at the interface between the electrode and the ambient. For gold surfaces up to $T_i = 60\ ^oC$, the net heat of adsorption is small, i.e. $Q_i \approx Q_v$. In this temperature range M_W primarily depends on the relative humidity; $M_W \approx \frac{RH}{1-RH}$ [14]. Since increasing T_{atm} will increase the dew-point and hence reduce the ambient RH as shown in $Fig. 2\ (c)$, the number of adsorbed monolayers will decrease. It should also be noted that since the device is heated from below, T_i is always larger than T_{atm} causing M_W to be lower at the interface. Since c will decrease exponentially with T_i, M_W and therefore the degradation rate, will decrease as is presently observed. On the other hand, if the device was heated from above by the ambient the degradation rate would be expected to increase. Below $60\ ^oC$, at higher RH-values the adsorbed water will due to horizontal interactions form a surface film causing the number of adsorbed molecules to depart from that predicted by BET-theory. Also, it can be mentioned that the amount of adsorbed water molecules will also change depending on the composition and cleanliness of the surfaces being studied [14].

These literature findings correlate well with the current measured increasing cycles to failure with increasing T_{sub} (see *Fig. 2* (c) and *TABLE I*). This may suggest that the design of the reliability-experiment, such as the relation between the device temperature and the ambient temperature, the absolute ambient humidity, the cleanliness of the device being tested etc., may to a large extent dictate the outcome of lifetime and reliability tests. It can for example be noted that no local breakdown-events was observed for devices operated at $RH = 35\ \%$ at $T_{sub} = 25\ ^oC$, and $T_{atm} = 25\ ^oC$ for up to $1.5x10^{11}$ cycles. At $T_{sub} = 175\ ^oC, T_{atm} = 62.3\ ^oC$ and $RH = 15.4\ \%$ on the other hand, failure occurred after $9x10^8$ cycles also due to humidity-related degradation.

The measured degradation deflection amplitude in high humidity was typically characterized by four sudden drops during operation, as shown in the inset of *Fig. 3* (b). Each drop was associated with the breach of an electrode routing connecting the wire-bonding pads to the actuating membrane. Hence, device failure was here defined as the breach of the first electrode. The tilt relative to the tilt at $25\ ^oC$ as a function cycles until the first routing breach is plotted vs T_{sub} in the main graph of *Fig. 3* (b). As seen, the deflection amplitude declines by cycling for all devices. But, even though the rate of decline was significantly higher at elevated temperatures, as to be expected [5], the lifetime was indeed longer as defined for the current devices. However, the electromechanical degradation by cycling was found to exceed the expected contribution from pure ferroelectric fatigue. E.g. at $175\ ^oC$ the average decrease in tilt was $65\ \%$ opposed to a $10\ \%$ decrease in P_S after $5x10^8$ cycles (not shown here). ε_r remained approximately constant throughout the experiments. Again, this points towards the in-plane sensitivity to film-substrate stress transfer and other factors of such devices. Lastly it can be mentioned that no short-circuiting was detected prior to the shown routing breaches.

IV. Summary and Conclusions

Unipolar temperature-humidity-cycling tests with a constant absolute humidity of $22\ g/m^3$ and substrate temperatures from 25^oC to $175\ ^oC$ were carried out to assess the lifetime and reliability of PZT-based piezoelectric micromirrors. For all temperatures, humidity related degradation by local breakdown-events was more pronounced and preceded that related to polarization fatigue. Also, the average initial piezoelectric response and number of cycles to device failure were both found to increase with increasing substrate temperatures.

Acknowledgments

The authors wish to thank A. Vogl, P. Wittendorp and J. Gjessing for their excellent scientific and technical support. The present research was kindly supported by the Research Council of Norway under contract number 247781/O30.

References

[1] C.-B. Eom and S. Trolier-McKinstry, "Thin-film piezoelectric MEMS," *MRS Bull.*, vol. 37, no. 11, pp. 1007–1017, 2012.

[2] T. Bakke et al., "A novel ultra-planar, long-stroke and low-voltage piezoelectric micromirror," *J. Micromechanics Microengineering*, vol. 20, p. 064010, 2010.

[3] I. P. Lipscomb et al., "The effect of relative humidity, temperature and electrical field on leakage currents in piezo-ceramic actuators under dc bias," *Sensors Actuators, A Phys.*, vol. 151, no. 2, pp. 179–186, 2009.

[4] H. Nazeer et al., "Residual stress and Young's modulus of pulsed laser deposited PZT thin films: Effect of thin film composition and crystal direction of Si cantilevers," *Microelectron. Eng.*, vol. 161, pp. 56–62, 2016.

[5] D. Damjanovic, "Ferroelectric, dielectric and piezoelectric properties of ferroelectric thin films and ceramics," *Reports Prog. Phys.*, vol. 61, no. 9, pp. 1267–1324, 1998.

[6] Y. A. Genenko et al., "Mechanisms of aging and fatigue in ferroelectrics," *Mater. Sci. Eng. B Solid-State Mater. Adv. Technol.*, vol. 192, no. C, pp. 52–82, 2015.

[7] M. W. Hooker, "Properties of PZT-Based Piezoelectric Ceramics Between -150 and 250 C," *Lockheed Martin Eng. Sci. Co.*, no. September, p. 28, 1998.

[8] V. M. Glazov and A. S. Pashinkin, "The Thermophysical Properties (Heat Capacity and Thermal Expansion) of Single-Crystal Silicon," *High Temp.*, vol. 39, no. 3, pp. 413–419, 2001.

[9] D. Zheng et al., "Multi-breakdown model for explaining the formation and growth of black spots in PZT capacitor under DC bias," *Sensors Actuators, A Phys.*, vol. 241, pp. 197–202, 2016.

[10] D. Zheng et al., "Current leakage and transients in ferroelectric ceramics under high humidity conditions," vol. 158, pp. 106–111, 2010.

[11] C. Huang et al., "Effect of hydrogen on Pb(Zr,Ti)O3-based ferroelectric capacitors," *J Appl Phys*, vol. 98, no. 98, p. 104105, 2005.

[12] G. M. Mullen et al., "The effects of adsorbed water on gold catalysis and surface chemistry," *Top. Catal.*, vol. 56, no. 15–17, pp. 1499–1511, 2013.

[13] J. M. Polfus et al., "Surface defect chemistry of Y-substituted and hydrated BaZrO 3 with subsurface space-charge regions," *J. Mater. Chem. A*, vol. 4, no. 19, pp. 7437–7444, 2016.

[14] S. Sharma and J. Thomas III, "Adsorption of water vapor on thin gold electroplated on copper," *J. Vac. Sci. Technol.*, vol. 825, pp. 3–5, 1977.

This template, modified in MS Word 2007 and saved as a "Word 97-2003 Document" for the PC, provides authors with most of the formatting specifications needed for preparing electronic versions of their papers. All standard paper components have been specified for three reasons: (1) ease of use when formatting individual papers, (2) automatic compliance to electronic requirements that facilitate the concurrent or later production of electronic products, and (3) conformity of style throughout a conference proceedings. Margins, column widths, line spacing, and type styles are built-in; examples of the type styles are provided throughout this document and are identified in italic type, within parentheses, following the example. Some components, such as multi-leveled equations, graphics, and tables are not prescribed, although the various table text styles are provided. The formatter will need to create these components, incorporating the applicable criteria that follow.

V. Ease of Use

A. Selecting a Template (Heading 2)

First, confirm that you have the correct template for your paper size. This template has been tailored for output on the A4 paper size. If you are using US letter-sized paper, please close this file and download the file "MSW_USltr_format".

B. Maintaining the Integrity of the Specifications

The template is used to format your paper and style the text. All margins, column widths, line spaces, and text fonts are prescribed; please do not alter them. You may note peculiarities. For example, the head margin in this template measures proportionately more than is customary. This measurement and others are deliberate, using specifications that anticipate your paper as one part of the entire proceedings, and not as an independent document. Please do not revise any of the current designations.

VI. Prepare Your Paper Before Styling

Before you begin to format your paper, first write and save the content as a separate text file. Keep your text and graphic files separate until after the text has been formatted and styled. Do not use hard tabs, and limit use of hard returns to only one return at the end of a paragraph. Do not add any kind of pagination anywhere in the paper. Do not number text heads-the template will do that for you.

Finally, complete content and organizational editing before formatting. Please take note of the following items when proofreading spelling and grammar:

A. Abbreviations and Acronyms

Define abbreviations and acronyms the first time they are used in the text, even after they have been defined in the abstract. Abbreviations such as IEEE, SI, MKS, CGS, sc, dc, and rms do not have to be defined. Do not use abbreviations in the title or heads unless they are unavoidable.

B. Units

- Use either SI (MKS) or CGS as primary units. (SI units are encouraged.) English units may be used as secondary units (in parentheses). An exception would be the use of English units as identifiers in trade, such as "3.5-inch disk drive."
- Avoid combining SI and CGS units, such as current in amperes and magnetic field in oersteds. This often leads to confusion because equations do not balance dimensionally. If you must use mixed units, clearly state the units for each quantity that you use in an equation.
- Do not mix complete spellings and abbreviations of units: "Wb/m2" or "webers per square meter," not "webers/m2." Spell units when they appear in text: "...a few henries," not "...a few H."
- Use a zero before decimal points: "0.25," not ".25." Use "cm3," not "cc." (*bullet list*)

C. Equations

The equations are an exception to the prescribed specifications of this template. You will need to determine whether or not your equation should be typed using either the Times New Roman or the Symbol font (please no other font). To create multileveled equations, it may be necessary to treat the equation as a graphic and insert it into the text after your paper is styled.

Number equations consecutively. Equation numbers, within parentheses, are to position flush right, as in (1), using a right tab stop. To make your equations more compact, you may use the solidus (/), the exp function, or appropriate exponents. Italicize Roman symbols for quantities and variables, but not Greek symbols. Use a long dash rather than a hyphen for a minus sign. Punctuate equations with commas or periods when they are part of a sentence, as in

$$a + b = \gamma \qquad (1)$$

$$\alpha + \beta = \chi. \qquad (1)$$

(1) (1)

Note that the equation is centered using a center tab stop. Be sure that the symbols in your equation have been defined before or immediately following the equation. Use "(1)," not "Eq. (1)" or "equation (1)," except at the beginning of a sentence: "Equation (1) is ..."

D. Some Common Mistakes

- The word "data" is plural, not singular.
- The subscript for the permeability of vacuum μ_0, and other common scientific constants, is zero with subscript formatting, not a lowercase letter "o."
- In American English, commas, semi-/colons, periods, question and exclamation marks are located within quotation marks only when a complete thought or name is cited, such as a title or full quotation. When quotation marks are used, instead of a bold or italic typeface, to highlight a word or phrase, punctuation should appear outside of the quotation marks. A parenthetical phrase or

Identify applicable sponsor/s here. If no sponsors, delete this text box (*sponsors).*

statement at the end of a sentence is punctuated outside of the closing parenthesis (like this). (A parenthetical sentence is punctuated within the parentheses.)

- A graph within a graph is an "inset," not an "insert." The word alternatively is preferred to the word "alternately" (unless you really mean something that alternates).
- Do not use the word "essentially" to mean "approximately" or "effectively."
- In your paper title, if the words "that uses" can accurately replace the word using, capitalize the "u"; if not, keep using lower-cased.
- Be aware of the different meanings of the homophones "affect" and "effect," "complement" and "compliment," "discreet" and "discrete," "principal" and "principle."
- Do not confuse "imply" and "infer."
- The prefix "non" is not a word; it should be joined to the word it modifies, usually without a hyphen.
- There is no period after the "et" in the Latin abbreviation "et al."
- The abbreviation "i.e." means "that is," and the abbreviation "e.g." means "for example."

An excellent style manual for science writers is [7].

VII. Using the Template

After the text edit has been completed, the paper is ready for the template. Duplicate the template file by using the Save As command, and use the naming convention prescribed by your conference for the name of your paper. In this newly created file, highlight all of the contents and import your prepared text file. You are now ready to style your paper; use the scroll down window on the left of the MS Word Formatting toolbar.

A. Authors and Affiliations

The template is designed so that author affiliations are not repeated each time for multiple authors of the same affiliation. Please keep your affiliations as succinct as possible (for example, do not differentiate among departments of the same organization). This template was designed for two affiliations.

1) For author/s of only one affiliation (Heading 3): To change the default, adjust the template as follows.

a) Selection (Heading 4): Highlight all author and affiliation lines.

b) Change number of columns: Select the Columns icon from the MS Word Standard toolbar and then select "1 Column" from the selection palette.

c) Deletion: Delete the author and affiliation lines for the second affiliation.

2) For author/s of more than two affiliations: To change the default, adjust the template as follows.

a) Selection: Highlight all author and affiliation lines.

b) Change number of columns: Select the "Columns" icon from the MS Word Standard toolbar and then select "1 Column" from the selection palette.

c) Highlight author and affiliation lines of affiliation 1 and copy this selection.

d) Formatting: Insert one hard return immediately after the last character of the last affiliation line. Then paste down the copy of affiliation 1. Repeat as necessary for each additional affiliation.

e) Reassign number of columns: Place your cursor to the right of the last character of the last affiliation line of an even numbered affiliation (e.g., if there are five affiliations, place your cursor at end of fourth affiliation). Drag the cursor up to highlight all of the above author and affiliation lines. Go to Column icon and select "2 Columns". If you have an odd number of affiliations, the final affiliation will be centered on the page; all previous will be in two columns.

B. Identify the Headings

Headings, or heads, are organizational devices that guide the reader through your paper. There are two types: component heads and text heads.

Component heads identify the different components of your paper and are not topically subordinate to each other. Examples include ACKNOWLEDGMENTS and REFERENCES, and for these, the correct style to use is "Heading 5." Use "figure caption" for your Figure captions, and "table head" for your table title. Run-in heads, such as "Abstract," will require you to apply a style (in this case, italic) in addition to the style provided by the drop down menu to differentiate the head from the text.

Text heads organize the topics on a relational, hierarchical basis. For example, the paper title is the primary text head because all subsequent material relates and elaborates on this one topic. If there are two or more sub-topics, the next level head (uppercase Roman numerals) should be used and, conversely, if there are not at least two sub-topics, then no subheads should be introduced. Styles named "Heading 1," "Heading 2," "Heading 3," and "Heading 4" are prescribed.

C. Figures and Tables

1) Positioning Figures and Tables: Place figures and tables at the top and bottom of columns. Avoid placing them in the middle of columns. Large figures and tables may span across both columns. Figure captions should be below the figures; table heads should appear above the tables. Insert figures and tables after they are cited in the text. Use the abbreviation "Fig. 1," even at the beginning of a sentence.

TABLE I. TABLE STYLES

Table Head	Table Column Head		
	Table column subhead	***Subhead***	***Subhead***
copy	More table copy[a]		

[a.] Sample of a Table footnote. *(Table footnote)*

b.

Fig. 1. Example of a figure caption. *(figure caption)*

Figure Labels: Use 8 point Times New Roman for Figure labels. Use words rather than symbols or abbreviations when writing Figure axis labels to avoid confusing the reader. As an example, write the quantity "Magnetization," or "Magnetization, M," not just "M." If including units in the label, present them within parentheses. Do not label axes only with units. In the example, write "Magnetization (A/m)" or "Magnetization (A (m(1)," not just "A/m." Do not label axes with a ratio of quantities and units. For example, write "Temperature (K)," not "Temperature/K."

ACKNOWLEDGMENT *(Heading 5)*

The preferred spelling of the word "acknowledgment" in America is without an "e" after the "g." Avoid the stilted expression "one of us (R. B. G.) thanks ...". Instead, try "R. B. G. thanks...". Put sponsor acknowledgments in the unnumbered footnote on the first page.

REFERENCES

The template will number citations consecutively within brackets [1]. The sentence punctuation follows the bracket [2]. Refer simply to the reference number, as in [3]—do not use "Ref. [3]" or "reference [3]" except at the beginning of a sentence: "Reference [3] was the first ..."

We suggest that you use a text box to insert a graphic (which is ideally a 300 dpi resolution TIFF or EPS file with all fonts embedded) because this method is somewhat more stable than directly inserting a picture.

To have non-visible rules on your frame, use the MSWord "Format" pull-down menu, select Text Box > Colors and Lines to choose No Fill and No Line.

Number footnotes separately in superscripts. Place the actual footnote at the bottom of the column in which it was cited. Do not put footnotes in the reference list. Use letters for table footnotes.

Unless there are six authors or more give all authors' names; do not use "et al.". Papers that have not been published, even if they have been submitted for publication, should be cited as "unpublished" [4]. Papers that have been accepted for publication should be cited as "in press" [5]. Capitalize only the first word in a paper title, except for proper nouns and element symbols.

For papers published in translation journals, please give the English citation first, followed by the original foreign-language citation [6].

[1] G. Eason, B. Noble, and I.N. Sneddon, "On certain integrals of Lipschitz-Hankel type involving products of Bessel functions," Phil. Trans. Roy. Soc. London, vol. A247, pp. 529-551, April 1955. (*references*)

[2] J. Clerk Maxwell, A Treatise on Electricity and Magnetism, 3rd ed., vol. 2. Oxford: Clarendon, 1892, pp.68-73.

[3] I.S. Jacobs and C.P. Bean, "Fine particles, thin films and exchange anisotropy," in Magnetism, vol. III, G.T. Rado and H. Suhl, Eds. New York: Academic, 1963, pp. 271-350.

[4] K. Elissa, "Title of paper if known," unpublished.

[5] R. Nicole, "Title of paper with only first word capitalized," J. Name Stand. Abbrev., in press.

[6] Y. Yorozu, M. Hirano, K. Oka, and Y. Tagawa, "Electron spectroscopy studies on magneto-optical media and plastic substrate interface," IEEE Transl. J. Magn. Japan, vol. 2, pp. 740-741, August 1987 [Digests 9th Annual Conf. Magnetics Japan, p. 301, 1982].

[7] M. Young, The Technical Writer's Handbook. Mill Valley, CA: University Science, 1989.